

# Semi-Automatic Segmentation of Coronary Arteries in CT Images

Anja Lemic

Master's thesis  
2016:E13



**LUND UNIVERSITY**

Lund Institute of Technology  
Centre for Mathematical Sciences  
Mathematics

FACULTY OF ENGINEERING, LTH

MASTER'S THESIS

---

# Semi-Automatic Segmentation of Coronary Arteries in CT images

---

*Author:*  
Anja Lemic

*Supervisor:*  
Einar Heiberg  
Felicia Seemann  
*Examiner:*  
Kalle Åström

Cardiac MR group  
Department of Clinical Physiology

June 6, 2016



## *Abstract*

Coronary heart diseases is one of the biggest health problems in the world today. By segmenting the coronary arteries in medical images and examining them, important information about abnormal narrowing and plaque, which are main causes to these diseases, can be found. Manual segmentation of the coronary arteries are time consuming and dependent on the observer, which makes the need of automatic segmentation techniques apparent.

The aim of the thesis is to implement an accurate and time-efficient algorithm to segment coronary arteries in computed tomography (CT) images. To do this, a model based algorithm combined with a multiple hypothesis approach has been implemented. This was first done in 2D and tested on manually made phantoms. Later on the algorithm was expanded to 3D, tested on phantoms and also on CT images of human hearts.

The thesis has been performed for the company Medviso. Medviso has created a software for cardiovascular image analysis, called Segment. All the implementation in this thesis has been preformed in Segment.

The algorithm was validated using two different datasets obtained from the Rotterdam Coronary Artery Evaluation Framework [1]. Results from these show that the proposed method can be used to segment coronary arteries and that it, using only one user interaction, on average finds 64% of the sought for vessels with a tracking accuracy close to manual delineation.



# Populärvetenskaplig sammanfattning

## *Att skapa bilder av livets träd – kranskärlen*

*Hjärtattack är en av de vanligaste dödsorsakerna i världen idag. Genom att utlinjera kranskärlen kan man skapa en tredimensionell bild av dessa. Undersökning av denna bild skulle effektivt kunna leda till identifiering av förträngningar i kranskärlen, den ledande orsaken till hjärtattack. Vi presenterar i detta arbete en semi-automatisk metod för att skapa en sådan bild.*

Hjärt- och kärlsjukdomar är den vanligaste dödsorsaken i Sverige och en av de vanligaste dödsorsakerna i världen. Den vanligaste hjärt- och kärlsjukdomen är hjärtattack och 2013 drabbades ungefär 28 000 människor i Sverige av en hjärtattack. Hjärtattack innebär att man får en blodpropp i ett av kärlen som förser hjärtat med blod, kranskärlen. Det finns två huvudkranskärl, ett på höger och ett på vänster sida av hjärtat. Dessa båda förgrenar sig till ett myller av kärl, som tillsammans förser hela hjärtat med blod. Blodproppar uppstår på grund av något som kallas åderförkalkning. Åderförkalkning innebär att fett och kalk har ansamlats inuti kranskärlen och gjort dessa trängre och stelare vilket gör det svårare för blodet att passera. När det blir helt stopp får man en hjärtinfarkt.

Genom att ta bilder av kranskärlen och undersöka om det finns förkalkningar eller fettansamlingar kan man alltså få värdefull information om risken för att få hjärtinfarkt, utan att behöva utföra några kirurgiska ingrepp. Idag används så kallad CT-röntgen (röntgen i 3 dimensioner) ofta för att ta tredimensionella bilder av hjärtat som kan användas för att undersöka kranskärlen. För att lättare kunna genomföra undersökningarna skulle man i bilderna vilja utlinjera kranskärlen och på så sätt skapa en tredimensionell bild av bara dessa. Detta kan göras, och gjordes länge, för hand av experter inom området. Problemet är att det tar minst 3 timmar för en van läkare och ännu längre tid om man är ovan. Detta är kostsamt (både ur tids- och pengaaspekter) och också en metod som är beroende av vilken läkare som har markerat kranskärlen. Bilderna är svårtolkade och även bland de bästa läkarna varierar svaren.

I denna artikel vill vi därför presentera ett program som genom två klick i bilden (ett för starten av varje kranskärl) automatiskt ska utlinjera kranskärlen och sedan presentera en tredimensionell bild av dessa. Resultaten visar att algoritmen hittar ca två tredjedelar av kranskärlen och att dessa utlinjeras med nästan lika stor precision som utlinjeringar av experter inom området. Det finns även en funktion som låter användaren lägga till fler punkter, vilket skulle kunna hjälpa till att höja andelen kärl som hittas.

Genom vidare utveckling av algoritmen skulle detta kunna bli en resursbesparande lösning som också undgår problemet med att utlinjeringarna kan variera. Om man skickar in samma startpunkt och samma bild till programmet så kommer bilden som kommer ut alltid att vara den samma.



# Contents

<b>Abstract</b>	<b>iii</b>
<b>Popularvetenskaplig sammanfattning</b>	<b>v</b>
<b>List of abbreviations</b>	<b>ix</b>
<b>1 Introduction</b>	<b>1</b>
1.1 Thesis overview . . . . .	2
<b>2 Medical Background</b>	<b>3</b>
2.1 The heart . . . . .	3
2.1.1 Coronary arteries . . . . .	3
2.2 Myocardial infarction . . . . .	4
2.3 CT images of coronary arteries . . . . .	4
2.4 Software . . . . .	5
<b>3 Aim</b>	<b>7</b>
<b>4 Theory</b>	<b>9</b>
4.1 Tree structures . . . . .	9
4.2 Multiple hypothesis tracking . . . . .	9
4.3 Solving a weighted linear least squares problem . . . . .	12
4.3.1 Student's t-test to test the significance of $\hat{\beta}$ . . . . .	13
4.4 Spectral clustering . . . . .	13
<b>5 Method</b>	<b>15</b>
5.1 An overview of the algorithm . . . . .	15
5.2 Build tree . . . . .	16
1. Place seeding point . . . . .	17
2. Create a vessel template . . . . .	17
3. Sample predictions . . . . .	19
4. Calculate score . . . . .	22
5. Choose best predictions . . . . .	22
5.3 Evaluate tree . . . . .	23
1. Calculate a branch score . . . . .	24
2. Bifurcation . . . . .	25
3. Choose branch . . . . .	28
4. Build new tree . . . . .	28
5.4 Interpolate . . . . .	28
<b>6 Validation</b>	<b>29</b>
6.1 Validation data . . . . .	29
6.2 Tracking ability . . . . .	29
6.2.1 Dataset 1- ability to find vessels . . . . .	30
6.2.2 Dataset 2 - ability to track the whole vessel . . . . .	30



6.3	Tracking accuracy . . . . .	31
<b>7</b>	<b>Results</b>	<b>33</b>
7.1	Phantoms . . . . .	33
7.2	Tracking ability . . . . .	35
7.2.1	Dataset 1- ability to find vessels . . . . .	35
7.2.2	Dataset 2 - ability to track the whole vessel . . . . .	37
7.3	Tracking accuracy . . . . .	39
<b>8</b>	<b>Discussion and Conclusions</b>	<b>41</b>
8.1	Discussion . . . . .	41
8.1.1	Limitations . . . . .	43
8.1.2	Future work . . . . .	44
8.2	Conclusions . . . . .	44
	<b>Bibliography</b>	<b>47</b>

# List of Abbreviations

<b>CT</b>	<b>Computed Tomography</b>
<b>MR</b>	<b>Magnetic Resonance</b>
<b>CMR</b>	<b>Cardiac Magnetic Resonance</b>
<b>MHT</b>	<b>Multiple Hypothesis Tracking</b>
<b>SD</b>	<b>Standard Deviation</b>
<b>TP</b>	<b>True Positives</b>
<b>FP</b>	<b>False Positives</b>
<b>FN</b>	<b>False Negatives</b>
<b>OV</b>	<b>Overlap</b>
<b>RMSE</b>	<b>Root Mean Square Error</b>
<b>SCAPIS</b>	<b>Swedish CardioPulmonary bioImage Study</b>



# Chapter 1

## Introduction

Cardiovascular diseases affects 1.4 million people in Sweden and is the most common cause of death in Sweden today [2] and one of the leading causes of death worldwide [3]. In the year of 2013 approximately 28 000 people in Sweden had a myocardial infarction, commonly known as heart attack, and of these 7 700 died. The research and medical care within the field has been very successful the last 30 years which has led to a great reduction in the number of myocardial infarctions and their deadly outcome has been reduced to half [4]. Still, myocardial infarction is one of the leading causes to premature death in Sweden.

Myocardial infarction is the caused by a thrombosis created in one of the blood vessels supplying the heart with blood, the coronary arteries. Because of the magnitude and deadly outcome of this disease the demand for improved diagnostic tools for analyzing the coronary arteries is high. The introduction of different medical imaging modalities has introduced a new, noninvasive way, of diagnosing patients. The use of computed tomography (CT) imaging has, due to its sensitivity, proven to be a very helpful tool for analyzing coronary arteries.

To be able to make quantitative analysis of the coronary arteries, a way of localizing and extracting them is needed. This is called segmentation. The segmentation could be obtained from manual delineation by specialists within the field or by automatic or semi-automatic methods. The problem with manual segmentation of the coronary arteries is that it is dependent of the observer and also a very time consuming –and thus expensive– way of localizing the vessels in the images. This is why reliable automatic methods for segmenting coronary arteries are needed.

Today there are many different approaches and algorithms used to automatically segment different types of vessels within the human body. But because of the low contrast in the area of coronary arteries, their proximity to other bigger vessels like the aorta and the fact that they are very thin makes segmenting coronary arteries a difficult task where algorithms produced for segmenting other vessels are of little help.

During the last decade a variety of different techniques for segmenting coronary arteries has been presented. These can be divided in to two main categories; vessel enhancement methods and vessel segmentation methods.

The vessel enhancement methods try to enhance the appearance of the coronary arteries in the images by different techniques e.g. by removing background structures. The other category, the vessel segmentation methods, come in many forms. They can be based on pattern recognition, model-based tracking and propagation, neural networks, artificial intelligence-based methods etc.[5].

This thesis has been performed for the company Medviso, in collaboration with the department of Clinical Physiology in Lund. Medviso has developed a software for cardiovascular image analysis called Segment. Segment was initially developed for Magnetic Resonance (MR) images, but has since then expanded to also include CT images. At the start of this thesis there was a desire for a method that could segment coronary arteries in Segment but no algorithm or implementation for it.

## **1.1 Thesis overview**

Chapter 2 contains a short medical background about the heart and the coronary arteries. It also includes background about CT images of coronary arteries and the software Segment. Chapter 3 presents the aim of the thesis. Chapter 4 contains theory. Chapter 5 presents the method used. In Chapter 6 the validation data and methods are presented, Chapter 7 contains the results and Chapter 8 contains conclusions and discussion.

## Chapter 2

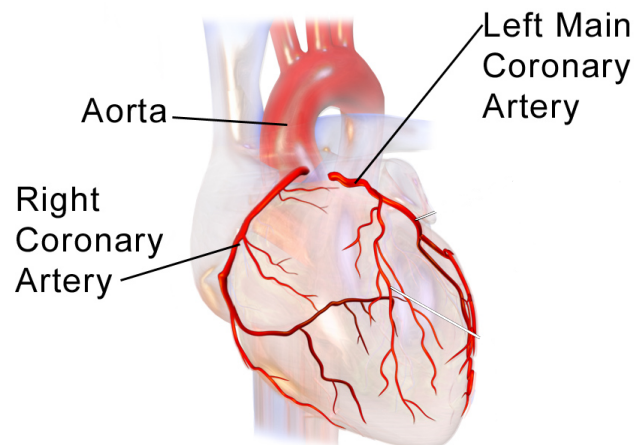
# Medical Background

### 2.1 The heart

The heart is a muscular organ inside the body that has a vital function; to pump the blood of the body. By pumping the blood through the vessels, which are part of the body's circulatory system, the heart provides the body with oxygen and nutrients meanwhile helping in the process of removing harmful metabolic waste. The heart needs to supply the same service to itself and it does this through the coronary vessels [6].

#### 2.1.1 Coronary arteries

The coronary arteries are the vessels that deliver oxygenated blood to the heart muscle. There are two main coronary arteries, the right and the left, and both originate from the root of the aorta. The two main coronary arteries both branch off in to a tree of vessels, see Figure 2.1, in order to support the whole heart with blood [6].



### Coronary Arteries

FIGURE 2.1: Illustration of a human heart and the coronary arteries [7].

## 2.2 Myocardial infarction

Myocardial infarction is when a part of the heart muscle is damaged due to insufficient coronary blood flow. The most common cause of myocardial infarction is the rupture of an atherosclerosis plaque. Atherosclerosis is when an artery wall thickens due to fats and inflammatory cells that are stored inside the vessel walls [8]. When the atherosclerotic plaque ruptures its content gets in contact with the blood and makes it clot; a thrombosis is created. Hence, the amount of plaque as well as plaque composition inside the coronary arteries and possible thickenings to the artery walls could provide important information about the risk of getting a myocardial infarction. [6]

## 2.3 CT images of coronary arteries

Computed tomography, CT, is a common tool used in medical facilities for producing medical images and could be seen as a 3D version of an X-ray image. The images produced by the CT scanner allows the user to see the inside of an object without invasive techniques. Before computing the CT images the patients receive an iodine-containing contrast material as an injection to ensure the best possible images of the coronary arteries. Figure 2.2 shows four different 2D sections of a CT image of a human heart. The images are displayed in the transversal plane with a feet-head view. A way of visualizing the transversal plane is to think of it as the patient is laying on his/her back and one is viewing a cross section of the heart standing by the patients feet looking towards the head. In each of the images the coronary arteries has been indicated by arrows.

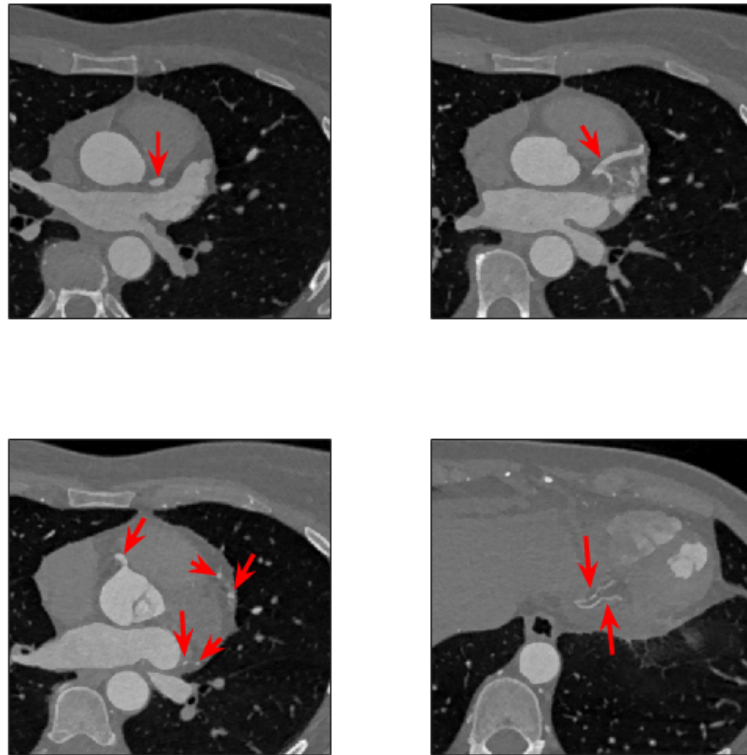


FIGURE 2.2: Example of coronary arteries in CT images of a human heart. The coronary arteries are indicated by the red arrows.

## 2.4 Software

The medical software Segment is provided by the company Medviso. Medviso was founded 2007 by Einar Heiberg as a spinn-off to his research in the Lund Cardiac MR group. Segment is freely available for research purposes but not for clinical use [9]. There are two clinical versions of Segment, Segment CMR and Segment CT. Segment CMR is the first version of Segment and is developed mainly for cardiovascular magnetic resonance imaging. Segment CT is a later release of Segment and has been developed for CT images. However, Segment CMR and Segment CT share the same platform so the algorithms are reachable from both versions of the software. Both versions of Segment are mainly implemented in Matlab.





## Chapter 3

### Aim

The aim of this masters thesis is to develop a semi-automatic algorithm for segmenting coronary arteries in CT images. The algorithm should be implemented in the software Segment and the results should be validated, both for tracking ability and tracking accuracy.

The specific aims of this masters thesis are to

- Develop a semi-automatic algorithm for segmenting coronary arteries in CT images.
- Validate the performance of the algorithm in CT images of human hearts.
- Implement the algorithm in the software Segment.



## Chapter 4

# Theory

### 4.1 Tree structures

A tree is a hierarchical data structure used to make the accessing and sorting of data easier. Every node in a tree has exactly one parent, except for the first node, and no or several children. An example of a tree structure can be seen in Figure 4.1.

Some terminology that is often used when working with tree structures are *root*, *leaf*, *branch* and *depth*. The root of a tree structure is the first node of the tree, in Figure 4.1 this is node 1. A leaf is a node without children. In Figure 4.1 nodes 4, 7, 8 and 9 are leaves and each path leading to a leaf is called a branch. Furthermore, the depth of a tree is how many nodes there is between the root and the leaf (including the leaf itself) of the longest branch. The tree in Figure 4.1 is of depth 3.

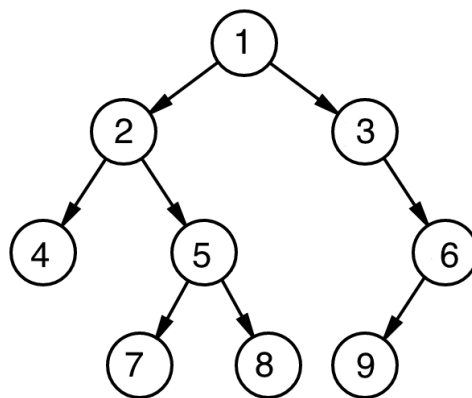


FIGURE 4.1: Example of a tree structure of depth 3. Node 1 is the root of the tree and node 4, 7, 8 and 9 are leaves.

### 4.2 Multiple hypothesis tracking

Multiple Hypothesis Tracking (MHT) is a method that was first proposed in 1979 [10]. The method has been popular within radar target tracking and visual tracking problems. The strength of the model is that it investigates multiple possible paths before making a decision which often results in a better overall performance. One of the disadvantages is that it can be slow and memory intensive [10].

The Multiple Hypothesis Tracking approach is to build a tree of potential

track hypothesis for each possible prediction and evaluating these by the likelihood of each track. The algorithm then returns the most likely combination of tracks as a solution.

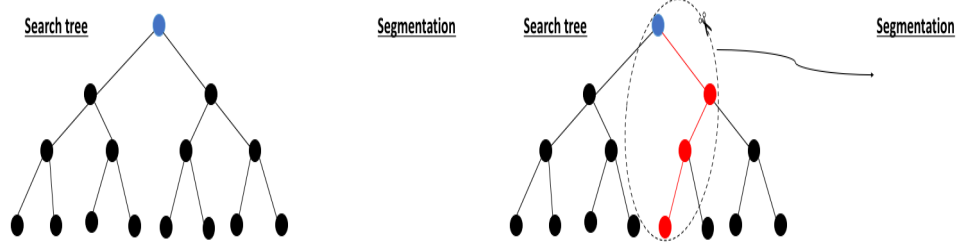
To avoid storing *all* possible paths forward (which is usually an enormous amount of data) and thus reduce the complexity of the model, different approaches have been introduced.

One approach often used is called pruning, this means that predictions that are not good enough are discarded. One great challenge with multiple hypothesis tracking algorithms is to find a quick and reliable way of pruning the tree in order to keep the number of track hypothesis manageable.

Another approach is to restrict the depth of the tree and evaluate the predicted paths forward more often. This is done by first building a small tree of a pre-defined depth, evaluated it to find the most likely path forward and then take a step towards this prediction. Then, a new small tree of predictions is built up, evaluated and a new step is taken. The algorithm continues until the problem has been solved.

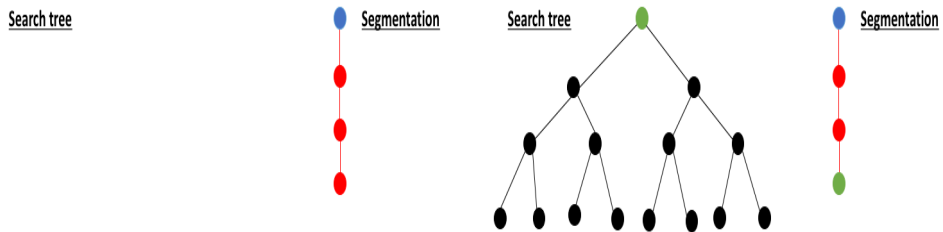
A graphical example of a multiple hypothesis tracking approach where the depth of the tree has been restricted to 3 can be seen in Figure 4.2.

In Figure 4.2A the first tree of depth 3 is built from the initial point (indicated in blue). In Figure 4.2B the tree has been evaluated and the best path has been found (indicated in red). This branch is stored (Figure 4.2C). From the leaf of this branch a new tree of depth 3 is built, seen in Figure 4.2D. This is evaluated and the best path is saved together with the first (Figure 4.2E). This procedure is continued until the problem has been solved (Figure 4.2F).



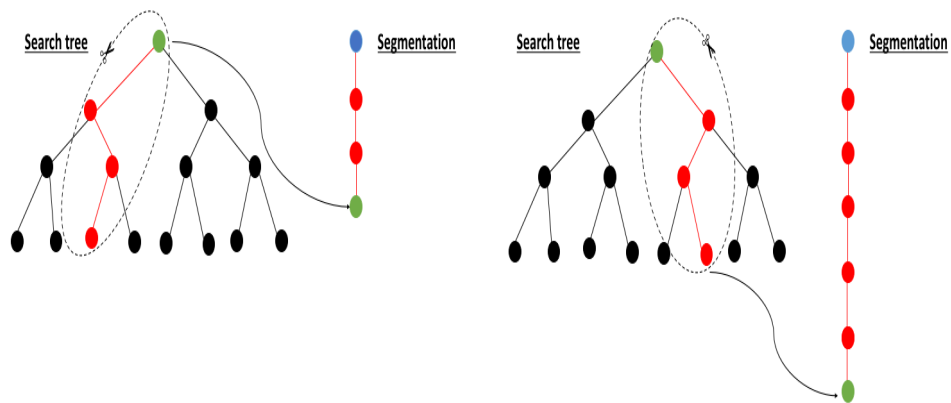
(A) A tree of depth 3 is built from the initial point (blue)

(B) The search tree is evaluated and the best path is found (red)



(C) The best path is stored in the segmentation

(D) A new tree of depth 3 is built from the last prediction in the segmentation



(E) The tree is evaluated and the best path is stored

(F) The search continues until the problem is solved

FIGURE 4.2: A graphical representation of a Multiple Hypothesis Tracking algorithm

### 4.3 Solving a weighted linear least squares problem

The method of least squares is a standard approach within regression analysis. It is often used to find the best fit of parameters when fitting a model to observed data. The best fit in the least squares sense are the parameters that minimize the sum of squared residuals, where the residual is the difference between the observed data and the model.

Assume a model defined as

$$Y_i = \beta_0 + \beta_1 X_i + \varepsilon_i \quad i = 1, \dots, n,$$

where  $\varepsilon_i \sim N(0, \sigma^2/w_i)$  for known constants  $w_i, \dots, w_n$ .

We now want to solve the following weighted least squares problem

$$\min_{\beta} \mathbf{S}(\beta) = \min_{\beta} \|\mathbf{W} \cdot (\mathbf{Y} - \mathbf{X}\beta)\|^2 \quad (4.1)$$

where

$$\mathbf{Y} = \begin{bmatrix} y_1 \\ \vdots \\ y_n \end{bmatrix}, \quad \mathbf{X} = \begin{bmatrix} 1 & x_1 \\ \vdots & \vdots \\ 1 & x_n \end{bmatrix}, \quad \beta = \begin{bmatrix} \beta_0 \\ \beta_1 \end{bmatrix}, \quad \mathbf{W} = \begin{bmatrix} w_1 & 0 & \cdots & 0 \\ 0 & w_2 & & \vdots \\ \vdots & & \ddots & 0 \\ 0 & & & w_n \end{bmatrix}.$$

This can be done by first expanding the expression within the norm in Equation (4.1) as

$$\begin{aligned} \mathbf{S}(\beta) &= \|\mathbf{W} \cdot (\mathbf{Y} - \mathbf{X}\beta)\|^2 \\ &= (\mathbf{W}(\mathbf{Y} - \mathbf{X}\beta))^T (\mathbf{W}(\mathbf{Y} - \mathbf{X}\beta)) \\ &= (\mathbf{Y}^T \mathbf{W}^T - \beta^T \mathbf{X}^T \mathbf{W}^T) (\mathbf{W}\mathbf{Y} - \mathbf{W}\mathbf{X}\beta) \\ &= \mathbf{Y}^T \mathbf{W}^T \mathbf{W}\mathbf{Y} - \mathbf{Y}^T \mathbf{W}^T \mathbf{W}\mathbf{X}\beta - \beta^T \mathbf{X}^T \mathbf{W}^T \mathbf{W}\mathbf{Y} \\ &\quad + \beta^T \mathbf{X}^T \mathbf{W}^T \mathbf{W}\mathbf{X}\beta. \end{aligned} \quad (4.2)$$

By noticing that the second term after the last equality,  $\mathbf{Y}^T \mathbf{W}^T \mathbf{W}\mathbf{X}\beta$ , has the dimension  $1 \times 1$  and is thus its own transpose (which is the third term after the last equality) the expression in Equation 4.2 can be further simplified as

$$\mathbf{S}(\beta) = \mathbf{Y}^T \mathbf{W}^T \mathbf{W}\mathbf{Y} - 2\beta^T \mathbf{X}^T \mathbf{W}^T \mathbf{W}\mathbf{Y} + \beta^T \mathbf{X}^T \mathbf{W}^T \mathbf{W}\mathbf{X}\beta. \quad (4.3)$$

The minimization of  $\mathbf{S}(\beta)$  with respect to  $\beta$  can be obtained by differentiating the expression from Equation (4.3) with respect to  $\beta$  and setting it equal to zero, i.e.

$$\frac{d}{d\beta} \mathbf{S}(\beta) = (\mathbf{X}^T \mathbf{W}^2 \mathbf{X})\beta - \mathbf{X}^T \mathbf{W}^2 \mathbf{Y} = 0, \quad (4.4)$$

where  $\mathbf{W}^T \mathbf{W} = \mathbf{W}^2$  is true because  $\mathbf{W}$  is a diagonal matrix.

Solving Equation 4.4 gives the optimal estimation of  $\beta$  as

$$\hat{\beta} = (\mathbf{X}^T \mathbf{W}^2 \mathbf{X})^{-1} \mathbf{X}^T \mathbf{W}^2 \mathbf{Y}. \quad (4.5)$$

### 4.3.1 Student's t-test to test the significance of $\hat{\beta}$

A Student's t-test is a statistical test which can be used to test if two sets of data are significantly different from each other. Within linear regression it is often used to test if an acquired coefficient,  $\hat{\beta}$ , is significantly different from zero.

The student's t-test to test if the estimated coefficient  $\hat{\beta}$  from the weighted linear regression fitting in Equation 4.5 is significantly different from zero is defined as

$$t_{score} = \frac{\hat{\beta} - 0}{std(\hat{\beta})} = \frac{\hat{\beta}}{std(\hat{\beta})}, \quad (4.6)$$

where  $std(\hat{\beta})$  is the standard error of  $\beta$ . It can be shown ([11]) that the standard error is obtained as

$$std(\beta) = \sqrt{\sigma^2 (\mathbf{X}^T \mathbf{W}^2 \mathbf{X})^{-1} \mathbf{X}^T \mathbf{W}^4 \mathbf{X} (\mathbf{X}^T \mathbf{W}^2 \mathbf{X})^{-1}}$$

where  $\mathbf{Y}$ ,  $\mathbf{X}$  and  $\mathbf{W}$  can be found in Equation (4.1) and  $\sigma^2$  is the variance of  $\mathbf{Y}$ .

A  $t_{score} > 3$  can be considered significant assuming that the noise of the process is Gaussian and spatially independent. This corresponds to a significance level of 99.9%.

## 4.4 Spectral clustering

Spectral clustering is a method for dividing data into different clusters. The method uses a measurement of the similarity and through the following scheme it clusters the data [12]:

1. Given an enumerated set of data points create a similarity matrix,  $S$ , as a symmetric matrix (i.e.  $S_{ij} = S_{ji}$ ) where  $S_{ij} \geq 0$  is a measure of the similarity between data point  $i$  and  $j$ .
2. Create a diagonal matrix,  $\mathbf{D}_{ii} = \sum_j S_{ij}$ .
3. Create the Laplacian matrix  $\mathbf{L} = \mathbf{D} - \mathbf{S}$
4. Find the second smallest eigenvector,  $l_2$ , of  $\mathbf{L}$ .
5. The positions with positive values in  $l_2$  define the data points belonging to cluster one and the positions with negative values in  $l_2$  define the data points belonging to cluster two.





## Chapter 5

# Method

The algorithm chosen for segmenting coronary arteries is inspired by the article *Multiple hypothesis template tracking of small 3D vessel structures* by Friman et al. [13]. Both the algorithm presented by Friman et al. and the algorithm presented in this thesis are based on the same method but with implementational differences. One of these is that the algorithm described in this thesis has been implemented in the software Segment and thus needed to be adjusted to fit an already existing environment.

The proposed algorithm uses a vessel model to create and evaluate predictions and a multiple hypothesis tracking algorithm, restricted to a depth of 3, to find the best path forward. The final segmentation consists of a number of vessel segments put together. Each of these vessel segments is defined by its parameters;  $x_0$ ,  $r$  and  $\hat{v}$ , where  $x_0$  is the spatial position in the image,  $r$  its radius and  $\hat{v}$  its direction. This setup –the final segmentation consisting of several small segments defined by their parameters– allows the segmentation to change both radius and direction along each vessel.

The algorithm was first developed in 2D and tested on manually made phantoms. After this, the algorithm was expanded to 3D.

### 5.1 An overview of the algorithm

The algorithm iterates between building a tree of a depth 3 and then evaluating it. In the end of the evaluation it adds the best branch of the tree to the segmentation and starts over, building a new tree from the leaf of the chosen branch, evaluates it and adds the best branch to the segmentation and so on, until the whole vessel has been segmented, see Figure 5.1.

A description of how the two main processes “Build tree” and “Evaluate tree”, as well as the process “Interpolate”, are done can be found in the following sections. The sections start with a flow chart describing the main content of each process and then a more detailed description follows.

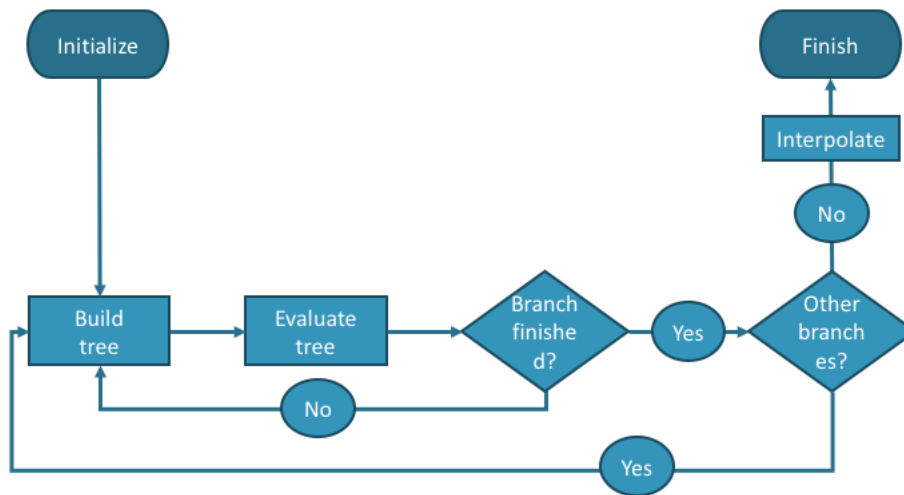


FIGURE 5.1: An overview of the algorithm.

## 5.2 Build tree

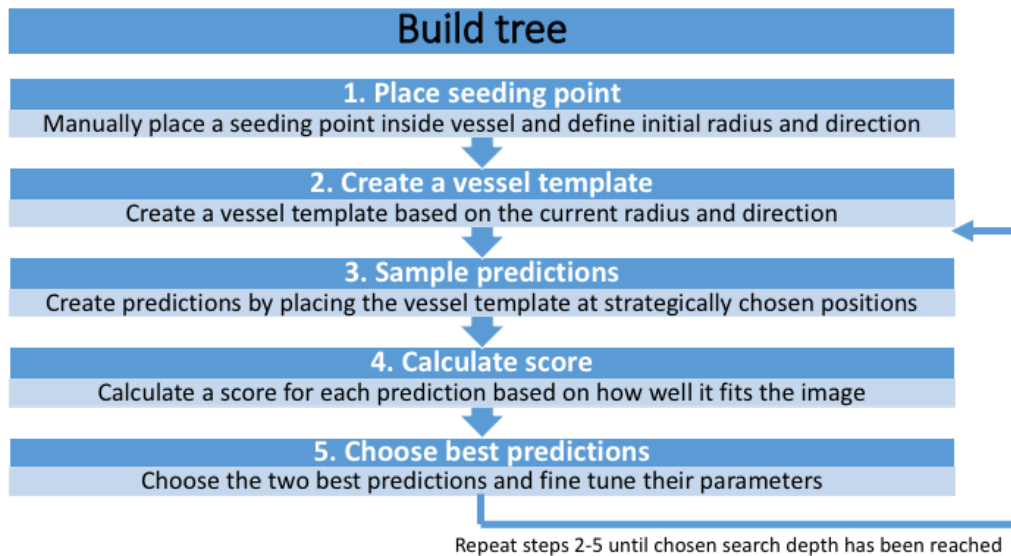


FIGURE 5.2: Flow chart explaining how each tree is created.

The subsections in this section describe how each of the five steps in the flowchart in Figure 5.2 is done in more detail. Each subsection starts with a short description of what happens in the step and after that a more detailed description follows. Together the subsections describe the whole process of how each tree is built.

### 1. Place seeding point

The seeding point is placed by the user with a mouse click in the image at a desirable position for the segmentation to start. The initial radius and direction is chosen by the user by specifying it as an input scalar and vector.

### 2. Create a vessel template

To be able to create a template of the vessel one first needs to decide on how to mathematically model the observed image. How this is done together with a description of how the vessel template function is defined can be found in this section.

#### Image model

The following image model was used to model a local surrounding  $x$  in the image,

$$I(\mathbf{x}) = kT(\mathbf{x}; r, \mathbf{x}_0, \hat{\mathbf{v}}) + m + \epsilon(\mathbf{x}), \quad (5.1)$$

where  $T(\mathbf{x}; r, \mathbf{x}_0, \hat{\mathbf{v}})$  is the vessel template model described below. The parameter  $k$  is the vessel contrast,  $m$  is the image background intensity and  $\epsilon(\mathbf{x})$  represents the noise in the image.

The parameters of the image model can be divided into two groups, image and vessel parameters. The image parameters,  $k$  and  $m$ , describe how the *intensities* in the image are modeled and the vessel parameters,  $\mathbf{x}_0$ ,  $r$  and  $\hat{\mathbf{v}}$ , describe how the *structure* of the vessel is modeled, i.e. its position, shape and direction.

#### How to define the vessel template model, $T(\mathbf{x}; r, \mathbf{x}_0, \hat{\mathbf{v}})$ ?

There are several ways one could create a model of a vessel. The vessel template model used is a combination of a vessel profile function,  $p$ , and a distance function,  $d^2$ , as

$$T(\mathbf{x}; r, \mathbf{x}_0, \hat{\mathbf{v}}) = p(d^2(\mathbf{x}; \mathbf{x}_0, \hat{\mathbf{v}}); r), \quad (5.2)$$

where  $x_0$  is the current spatial position,  $x$  is the local surrounding to  $x_0$ ,  $r$  is the current vessel radius and  $\hat{\mathbf{v}}$  is the current vessel direction.

The vessel profile function,  $p$ , describes which shape we expect the vessel to have. This mainly depends on if the data has been smoothed before the tracking begins. For smoothed data a "softer" profile function such as a Gaussian profile function is usually used. Smoothing of the data should be limited when tracking small structures such as the coronary arteries since this could remove important high frequency content in the image. Because of this the following "steeper" vessel profile function was used instead

$$p(d^2; r) = \frac{r^\gamma}{(d^2)^{\gamma/2} + r^\gamma}, \quad \gamma = 8$$

where  $\gamma$  is a parameter which controls the steepness of the function (this parameter was kept fixed in this project) and  $d^2$  is the distance function.

An example of how the profile function could look and a comparison with the Gaussian profile function can be seen in Figure 5.3.

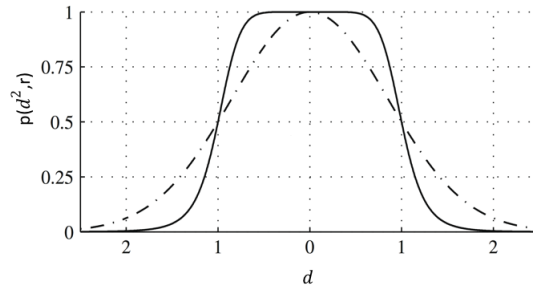


FIGURE 5.3: Example of how the profile function,  $p(d^2; r)$ , used in this thesis looks with  $r = 1$  and  $\gamma = 8$  (solid line). For comparison an equivalent Gaussian profile (dot-dashed line) has been plotted as well [13].

The distance function  $d^2$  used in this project is the squared distance to a line and is defined as follows

$$d^2(\mathbf{x}; \mathbf{x}_0, \hat{\mathbf{v}}) = \|\mathbf{x} - \mathbf{x}_0\|^2 - (\hat{\mathbf{v}}^T(\mathbf{x} - \mathbf{x}_0))^2.$$

A graphical explanation to how  $d^2$  is defined can be found in Figure 5.4.

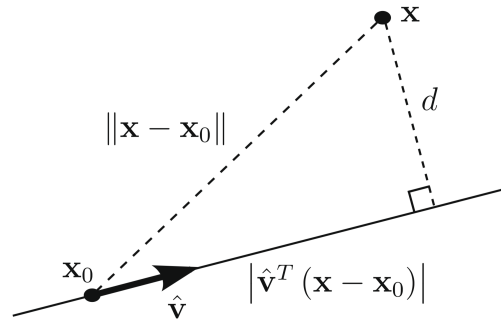


FIGURE 5.4: The distance  $d$  is the perpendicular distance between the point  $x$  and the line defined by the direction  $\hat{v}$  going through the point  $x_0$ . It can be found by using Pythagoras' theorem.

The vessel template defined in Equation (5.2),  $T(\mathbf{x}; r, \mathbf{x}_0, \hat{\mathbf{v}})$ , is designed so that it only takes values in the interval  $[0, 1]$ , where values close to 1 correspond to the vessel and values close to 0 correspond to background. An illustration of how this vessel template can look can be found in Figure 5.5.

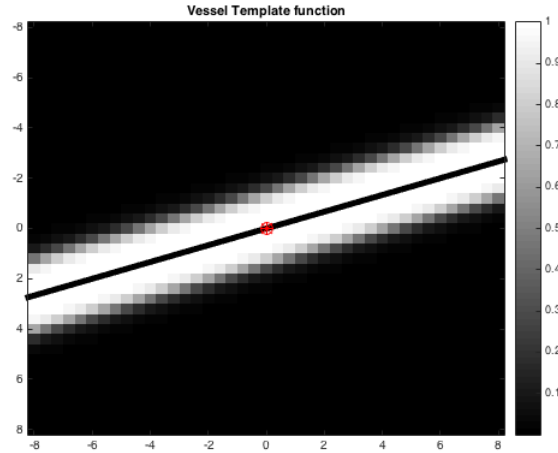


FIGURE 5.5: Example of how a vessel template used in this thesis could look in 2D. The red point is the current position and the black line indicates the vessel direction. The white pixels correspond to the vessel and the black pixels correspond to background.

### 3. Sample predictions

In this step an initial guess of spatial position, vessel direction and radius of the 7 predictions (in 2D) or 49 predictions (in 3D) is done. Then the image parameters  $k$  and  $m$  of the image model  $I(x)$ , found in Equation (5.1), are fitted to suit the observed image for each prediction.

To make sure that the fitting of the parameters is not disturbed by surrounding structures one needs to define how much of the pixels surrounding a position that should be included in the fitting. This is an important part since the coronary arteries are very small and surrounded by other high intensity objects in the image (such as the aorta). So, one would like to find a large enough surrounding to  $\mathbf{x}_0$  to capture the important information about the coronary artery in that spatial position but a small enough surrounding not to let the parameter fitting be disturbed by the intensities of surrounding bright structures.

Note that in this step it is only the image parameters,  $k$  and  $m$ , that are fitted to the observed data. The vessel parameters are, as mentioned before, guessed in this step and will later on be updated to suit the data better.

### How to find an initial guess of the predictions?

In this project the length of each step was decided by the current vessel radius  $r$ . Each prediction was placed at a distance of  $1.8 \cdot r$  from the current spatial position,  $x_0$ , and then modeled to have the same radius as  $x_0$ . Furthermore, instead of placing predictions all the way around  $x_0$  it was chosen to only make predictions in the current vessel direction  $\pm 70^\circ$ . An example of how predictions were placed in 2D can be found in figure 5.6

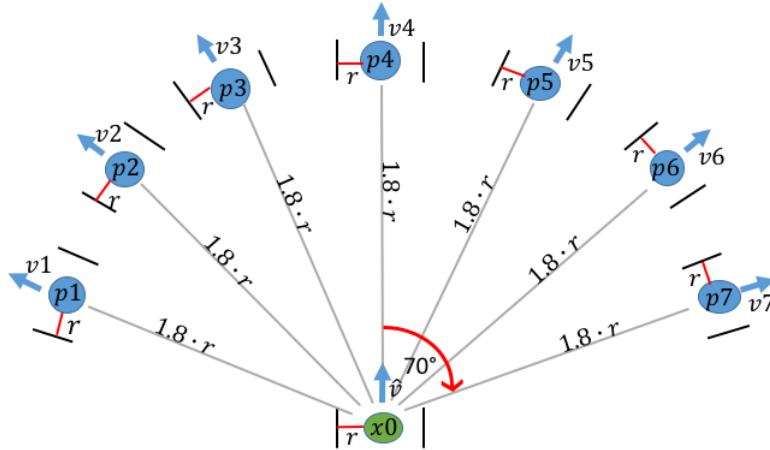


FIGURE 5.6: Example of how the sampling of predictions in 2D could look. The current position,  $x_0$ , can be seen as a green dot with the current vessel direction,  $\hat{v}$ , and the current radius,  $r$ . Each prediction (blue dot),  $p_1 \dots p_7$ , is sampled at a distance  $1.8 \cdot r$  from  $x_0$  in the directions  $v_1 \dots v_7$ . These directions are found as 7 directions evenly spaced between  $\hat{v} - 70^\circ$  and  $\hat{v} + 70^\circ$ .

### Which voxels are important to include when fitting parameters to observed data?

To decide how many voxels around a spatial position should be included when fitting parameters, a Gaussian weight function was used. The weight function is centered at  $\mathbf{x}_0$  and is defined as

$$w(\mathbf{x}; r, \mathbf{x}_0, \hat{\mathbf{v}}) = \exp\left(-\frac{\left(\hat{\mathbf{v}}^T(\mathbf{x} - \mathbf{x}_0)\right)^2}{(2r)^2} - \frac{\left(\hat{\mathbf{u}}_1^T(\mathbf{x} - \mathbf{x}_0)\right)^2 + \left(\hat{\mathbf{u}}_2^T(\mathbf{x} - \mathbf{x}_0)\right)^2}{(4r)^2}\right),$$

where  $\hat{\mathbf{v}}$ ,  $\hat{\mathbf{u}}_1$  and  $\hat{\mathbf{u}}_2$  are of unit length and orthogonal to each other.

How the weight function behaves can be seen in Figure 5.7. The voxels with a weight larger than 0.05 were used as the local surrounding,  $\mathbf{x}$ , to  $\mathbf{x}_0$  and only these voxels were considered when fitting the image parameters at this spatial position. One thing to notice about the weight function used is that it is broader over the vessel than along the vessel.

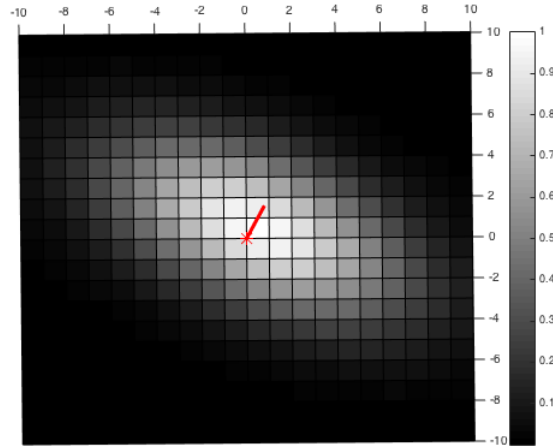


FIGURE 5.7: Example of how the weight function used in this thesis could look. The red dot indicates the current position,  $\mathbf{x}_0$ , and the red line indicates current vessel direction,  $\hat{\mathbf{v}}$ . Bright pixels correspond to a high weight and dark pixels to a low weight.

### Finding the image parameters $k$ and $m$

Fitting the image parameters found in Equation (5.1), i.e.  $k$  and  $m$ , to the observed image can be done by solving the following least squares problem:

$$\min_{k,m} \|\mathbf{W}(r, \mathbf{x}_0, \hat{\mathbf{v}}) \cdot (k\mathbf{T}(r, \mathbf{x}_0, \hat{\mathbf{v}}) + m\mathbf{1}_n - \mathbf{I})\|^2 \quad (5.3)$$

where  $\mathbf{I}$  and  $\mathbf{T}(r, \mathbf{x}_0, \hat{\mathbf{v}})$  contain the image data and template values for the local surrounding, i.e. the pixels with a weight larger than 0.05, to  $\mathbf{x}_0$  and  $\mathbf{W}(r, \mathbf{x}_0, \hat{\mathbf{v}})$  is a diagonal matrix with the weights of the local surrounding in its diagonal.

Since Equation (5.3) is linear in the image parameters a solution to this problem can be found similarly to what has been described in Section 4.3 *Solving a weighted linear least squares problem* in the following manner.

Keep the vessel parameters constant and introduce the following matrices

$$\mathbf{X} = \begin{bmatrix} T(\mathbf{x}_1; r, \mathbf{x}_0, \hat{\mathbf{v}}) & 1 \\ \vdots & \vdots \\ T(\mathbf{x}_n; r, \mathbf{x}_0, \hat{\mathbf{v}}) & 1 \end{bmatrix}, \quad \beta = \begin{bmatrix} k \\ m \end{bmatrix},$$

where  $n$  is the number of voxels in the surrounding to  $\mathbf{x}_0$ .

Equation (5.3) can now be written as

$$\begin{aligned} \min_{k,m} \|\mathbf{W}(r, \mathbf{x}_0, \hat{\mathbf{v}}) \cdot (k\mathbf{T}(r, \mathbf{x}_0, \hat{\mathbf{v}}) + m\mathbf{1}_n - \mathbf{I})\|^2 \\ = \\ \min_{k,m} \|\mathbf{W}(r, \mathbf{x}_0, \hat{\mathbf{v}}) \cdot (\mathbf{X}\beta - \mathbf{I})\|^2 \end{aligned} \quad (5.4)$$



By comparing the second expression in Equation 5.4 to Equation 4.1 it can be seen that the optimal image parameters can be found as

$$\begin{bmatrix} k \\ m \end{bmatrix} = (\mathbf{X}^T \mathbf{W}^2 \mathbf{X})^{-1} \mathbf{X}^T \mathbf{W}^2 \mathbf{I}.$$

#### 4. Calculate score

To be able to evaluate and compare different predictions each prediction was given a score. The score is based on the parameter  $k$  which describes the estimated vessel contrast. The score function was chosen to be the student's t-test to evaluate if  $k$  is significantly different from 0. If the vessel contrast is not significantly different from zero the image model in Equation 5.1 would be reduced to only background and noise, which means that the predictions should be rejected. Furthermore, the t-test can also be used to rank the predictions, a higher score corresponds to a better prediction.

The student's t-test for the image model parameter  $k$  can be written as [11]

$$score = \frac{k}{\sqrt{\sigma^2 \mathbf{c} (\mathbf{X}^T \mathbf{W}^2 \mathbf{X})^{-1} \mathbf{X}^T \mathbf{W}^4 \mathbf{X} (\mathbf{X}^T \mathbf{W}^2 \mathbf{X})^{-1} \mathbf{c}}},$$

where  $\mathbf{X}$  and  $\mathbf{W}$  are the same as in Equation 5.4,  $\mathbf{c} = \begin{bmatrix} 1 \\ 0 \end{bmatrix}$  is an indicator to extract information about the parameter  $k$  and  $\sigma^2$  is the variance of  $\mathbf{I}$ .

In the Section 4.3.1 Student's t-test to test the significance of  $\hat{\beta}$  it is stated that a t-score greater than 3 can be considered significant under the assumption that the image noise is Gaussian and uncorrelated. The noise in medical images are however, in general, not spatially independent. This will increase the t-score and a higher threshold for significance is needed. In this project the threshold for significance, called the pruning threshold, was chosen to be 10.

#### 5. Choose best predictions

To avoid keeping bad predictions all predictions with a score lower than the pruning threshold were rejected. If none of the predictions survived, the tracking of this branch was terminated. After this, the two (or one if only one survived) best predictions were kept and the vessel parameters of these were fine tuned to suit the observed data as good as possible. How this was done is described below.

##### Fine tuning the vessel parameters $r$ , $\mathbf{x}_0$ and $\hat{\mathbf{v}}$

The procedure to fine tune the vessel parameters is similar to what was done in *Finding the image parameters  $k$  and  $m$* . The same least squares problem was solved as before, but this time it was minimized over the vessel parameters, i.e.

$$\min_{r, \mathbf{x}_0, \hat{\mathbf{v}}} \|\mathbf{W}(r, \mathbf{x}_0, \hat{\mathbf{v}}) \cdot (k\mathbf{T}(r, \mathbf{x}_0, \hat{\mathbf{v}}) + m\mathbf{1}_n - \mathbf{I})\|^2 \quad (5.5)$$

where  $\mathbf{I}$ ,  $\mathbf{T}(r, \mathbf{x}_0, \hat{\mathbf{v}})$  and  $\mathbf{W}(r, \mathbf{x}_0, \hat{\mathbf{v}})$  are the same as in Equation (5.3).

After the change of parameters to optimize over, the problem in Equation (5.5) becomes nonlinear. Because of this, the sought after parameters are a little bit harder to find compared to before. In this thesis this was done by using the built in Matlab function `fminsearch`, which uses the Nelder-Mead simplex algorithm [14].

To prevent the function `fminsearch` from finding updates that were considered too far from the current values (this step is supposed to just "fine tune" the parameters, not make the spatial position jump to a different region of the image, make the vessel change direction or make the radius explode in size) some restrictions were made on the updates. The updated spatial position,  $x_0^{update}$ , was not allowed to be located more than 10 pixels from the old  $x_0$ . The updated direction was not allowed to vary more than  $\pm 30^\circ$  from the current vessel direction and the updated radius was not allowed to be larger than 15 pixels. If the update did not fulfill these restrictions, the old value was kept instead.

### 5.3 Evaluate tree

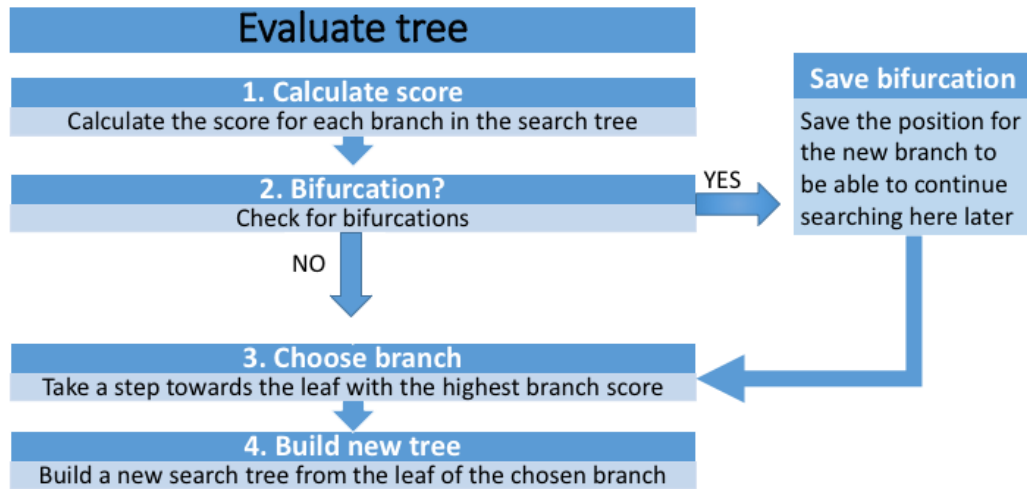


FIGURE 5.8: Flow chart explaining how each tree is evaluated.

In this section the steps of how each tree is evaluated (found in the flow chart in Figure 5.8) will be explained. In Figure 5.9 an example of a small tree of depth 1 can be seen. Each node is associated with a spatial position  $\mathbf{x}_0$ , a radius  $r$ , a direction  $\hat{\mathbf{v}}$ , a vessel contrast parameter  $k$ , a background intensity parameter  $m$  and a score.

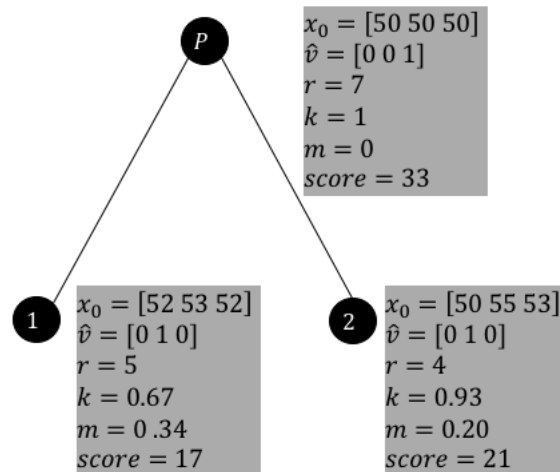


FIGURE 5.9: Example of how a tree could look.  $P$  indicates the starting node. The parameters associated with each node can be seen in the gray box.

### 1. Calculate a branch score

The branch score of each branch is the average score for the predictions on that branch, i.e. the score for each prediction summed and then divided with the number of nodes on the branch. This score was used to decide which branch was the best, but also to eliminate branches which are not good enough.

If the branch score of a branch was lower than a threshold, called elimination threshold, it was eliminated. The elimination threshold used was  $2 \cdot \text{pruningthres} = 20$ . The thresholds were used to make the algorithm faster but also to decide when to terminate. Without the pruning and termination thresholds the algorithm may continue indefinitely.

An example of how a search tree of depth 3 can look can be found in Figure 5.10. To make the figure a little easier only the score parameter of each prediction has been indicated (compared to all parameters in Figure 5.9). The branch score of each branch has also been indicated in the figure. Furthermore, some of the nodes have less than 2 children, this is due to the pruning threshold mentioned in Section 5. *Choose best predictions and fine tune them.*

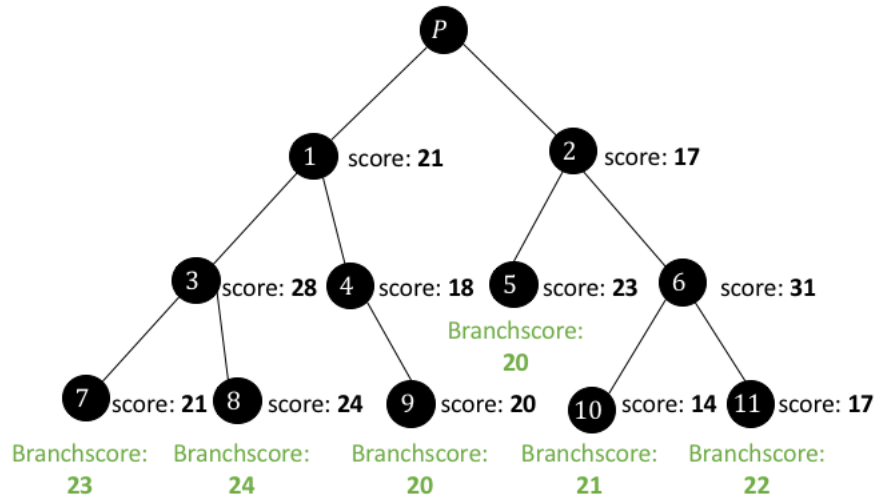


FIGURE 5.10: Example of how a search tree of depth 3 could look.  $P$  indicates the starting node. Each of the nodes 1-11 are one of the two best predictions in each step. The score of each prediction can be seen in black text and the branch score for each branch can be seen in green text.

## 2. Bifurcation

As described in Section 2.1.1 **Coronary arteries** there are two main coronary arteries which both branch in to a whole tree of vessels. So, it is important that the algorithm can detect bifurcations.

First, the leaves of the tracking tree was divided into two different clusters based on their spatial position and segmented radius. This was done using a spectral clustering algorithm described in Section 4.4 **Spectral clustering** with the similarity matrix,  $S$ , defined as

$$S_{ij} = S_{ji} = \exp\left(-2\frac{\|\mathbf{x}_i - \mathbf{x}_j\|}{r_i + r_j}\right), \quad i, j = 1 \dots n,$$

where  $\mathbf{x}_i$ ,  $\mathbf{x}_j$ ,  $r_i$  and  $r_j$  are the spatial coordinates and radius of leaf  $i$  and  $j$  and  $n$  is the number of leaves of the tree.

In Figure 5.11 the same search tree as in Figure 5.10 can be seen with the addition that the branches has been divided in to two clusters according to the scheme above.

The next step is to choose the leaves with the highest branch score within each cluster and find the distance between these two leaves. If the distance is larger than 1.7 times the current vessel radius a bifurcation has been detected.

In the example found in Figure 5.11 the leaves with highest branch score within each cluster are leaf 3 (node 8) and leaf 6 (node 11). The distance between leaves was calculated using the distance function presented in *How*

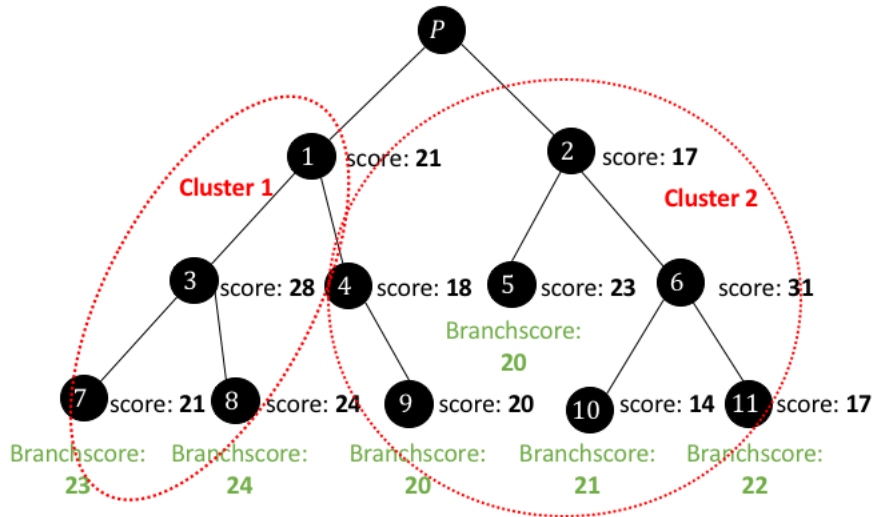


FIGURE 5.11: Example of a tree where the branches has been divided in two clusters. The branches associated with node 7 and 8 belong to cluster 1 and the branches associated with node 5, 9, 10 and 11 belong to cluster 2.

to define the vessel template model,  $T(\mathbf{x}; r, \mathbf{x}_0, \hat{\mathbf{v}})$ , i.e. by finding the perpendicular distance from one leaf's spatial position to the line going through the other leaf's spatial position with its vessel direction. This was done using the direction and spatial position of both leaves.

To make this more clear, a graphical example has been done. In Figure 5.12 the spatial position of leaf 3 has been indicated with a blue dot named  $p_1$ . The spatial position of leaf 6 has been indicated with a blue dot named  $p_2$ . The blue arrows are the predicted vessel directions associated with corresponding leaf. The first of the two sought for distances, call it  $d_1$ , can be found as the perpendicular distance between the line defined by  $p_2$ 's direction going through  $p_2$  and  $p_1$  (see Figure 5.12). In a similar manner the other distance,  $d_2$ , can be found as the perpendicular distance between the line going through  $p_1$  with corresponding direction and  $p_2$ . If either  $d_1$  or  $d_2$  is larger than  $1.7 \cdot r_P$ , where  $r_P$  is the radius of the current node  $P$  from Figure 5.10, a bifurcation is detected. An example of how this could look can be found in Figure 5.12.

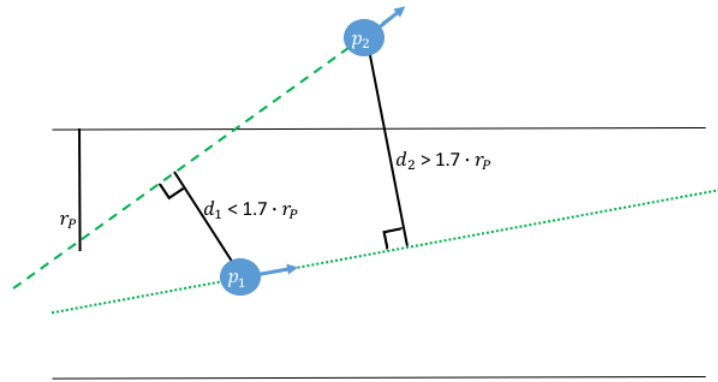


FIGURE 5.12: An example of the detection of a bifurcation. The black solid lines represent the borders of the vessel. The blue dots and arrows are the predictions spatial positions with the corresponding direction. The distance  $d_1$  is the perpendicular distance from the line going through  $p_2$  with  $p_2$ 's direction and  $p_1$ . The distance  $d_2$  is found similarly. The threshold for detection of a bifurcation is  $1.7 \cdot r_p$ , where  $r_p$  is the vessel radius of the current position. Since  $d_2 > 1.7 \cdot r_p$  a bifurcation has been detected.

This measurement of distance was used to avoid finding predictions located spatially far away from each other but in the same vessel direction, which could have happened if the distance would have been measured using e.g. the Euclidean distance. An example of this can be seen Figure 5.13, where the distances  $d_1$  and  $d_2$  are smaller than the threshold for detecting a bifurcation ( $1.7 \cdot r_p$ ), which means that no bifurcation was detected. The Euclidean distance (the red line in the figure) is larger than the threshold for bifurcation detection which would indicate that a bifurcation has been detected even though the predictions have apparently found the same vessel.

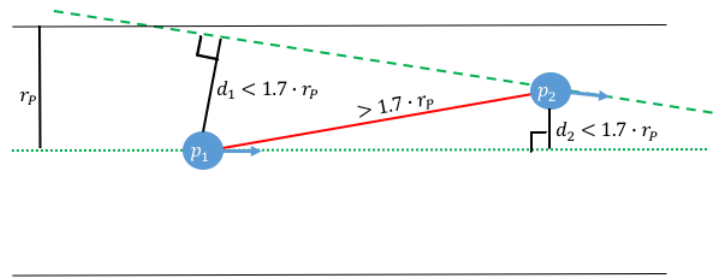


FIGURE 5.13: An example of why the chosen distance function has been used instead of the Euclidean distance (red line). The black solid lines represent the borders of the vessel. The blue dots and arrows are the predictions spatial positions and the corresponding direction. The threshold for detection of a bifurcation is  $1.7 \cdot r_P$ , where  $r_P$  is the vessel radius of the current position.

If a bifurcation was detected one of the branches was saved for further investigation later and then removed from the tree.

### 3. Choose branch

In this step the branch with the highest score was chosen to be added to the final segmentation.

### 4. Build new tree

The leaf of the branch added to the final segmentation was used as a starting position to build a new tree according to Section 5.2 **Build tree**.

## 5.4 Interpolate

As mentioned before, the final segmentation consisted of several segments with a spatial position, vessel direction and radius. To connect these segments an linear interpolation between each segment and its parent was done, for both the spatial position and the radius separately, and 3 new values were inserted. The number 3 was chosen because the average radius of the coronary vessels are, roughly approximated, 2 mm which would yield a distance between predictions at about 4 mm (they were sampled at  $1.8 \cdot r$ ). So, by inserting 3 interpolated values between each segmented point, the final segmentation has a distance of around 1 mm between points.

## Chapter 6

# Validation

During the development of the algorithm a dataset from the SCAPIS (Swedish CardioPulmonary bioImage Study) project obtained from Skåne University Hospital in Lund was used. The dataset consists of CT images from 7 patients.

The algorithm has been validated using two different datasets obtained from the Rotterdam Coronary Artery Algorithm Evaluation Framework [1]. Information about the datasets can be found in Section [6.1 Validation data](#).

The validation of the algorithm has been divided into two parts; tracking ability and tracking accuracy. The tracking ability has been validated using both datasets while the accuracy has been validated using just dataset 2. How the validation has been done is described in Section [6.2 Tracking ability](#) and Section [6.3 Tracking accuracy](#). The dataset were not used to calculate both tracking tracking ability and tracking accuracy because of the different content of the datasets. For all validation the segmentation with extra interpolated values was used.

### 6.1 Validation data

Dataset 1 consists of 9 patients where the whole tree of coronary arteries on both the left and right side of the heart has been manually marked and was used as reference standard. This dataset did not contain information about the radius of the coronary artery.

Dataset 2 consists of 8 patients with reference standard for four coronary arteries per patient, i.e. reference standard for 32 coronary arteries in total. The reference standard for dataset 2 contains the spatial position as well as the radius in each point of the coronary artery. It also includes inter-observer variability for the delineated radius in each point. The inter-observer variability reflects the variation between the results obtained by two or more observers examining the same material. In this evaluation framework the inter-observer variability was calculated as the root mean square error of three independent observers.

### 6.2 Tracking ability

The tracking ability was validated by two measurements. Dataset 1 was used to measure how many branches of the coronary arteries that was



found by the algorithm. Dataset 2 was used to measure the algorithms ability to track the whole vessel.

### 6.2.1 Dataset 1- ability to find vessels

The segmentation of each patient in Dataset 1 was visually validated by counting the number of branches that was found by the algorithm. These branches were further investigated to decide if the segmented branches were shorter, longer or the same length as the reference standard data. The branches were said to be of the same length if there were less than three predictions separating them.

### 6.2.2 Dataset 2 - ability to track the whole vessel

Dataset 2 was used to calculate a measurement called overlap, as has been described in the Rotterdam Coronary Artery Algorithm Evaluation Framework [1]. The overlap is similar to the well-known Dice coefficient [15] and is a measurement of the ability to track the complete vessel. To be able to define the overlap one first needs to define true positives, false negatives and false positives.

Every point in the *segmentation* can either be marked as a true positive,  $TP_{seg}$ , or a false positive,  $FP$ . A point in the segmentation is marked as true positive if there is at least one point in the reference standard at a distance less than the radius of that point, otherwise it is marked as false positive. Similarly, each point in the *reference standard* is defined as true positive,  $TP_{ref}$ , if the distance to at least one point in the segmentation is less than the radius of that point, otherwise it is defined as false negative,  $FN$ .

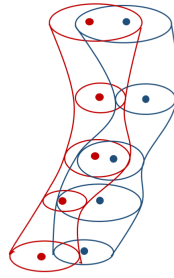
A graphical example describing true positives, false positives and false negatives can be found in Figure 6.1. In Figure 6.1 A an example of how the reference standard and segmentation could look can be found. Each point is the spatial position defining that segment and the circle surrounding it is the presumed radius. Each segment has been connected to form the final vessel. In Figure 6.1 B only the vessel representing the reference standard and the spatial positions of the segmentation has been plotted. In this figure it is shown how  $TP_{seg}$  and  $FP$  were obtained. In Figure 6.1 C the segmentation and spatial positions of the reference standard have been plotted to describe how  $TP_{ref}$  and  $FN$  were defined.

The overlap can now be defined as

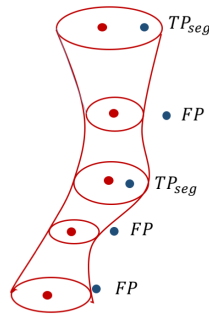
$$OV = \frac{||TP_{seg}|| + ||TP_{ref}||}{||TP_{seg}|| + ||TP_{ref}|| + ||FN|| + ||FP||}, \quad (6.1)$$

where  $|| \cdot ||$  denotes the amount of points marked as that type, e.g.  $||TP_{seg}||$  denotes the number of points in the segmentation that are marked as true positives. The overlap can vary in the interval  $[0,1]$ , where 0 corresponds to no overlap and 1 to perfect overlap.

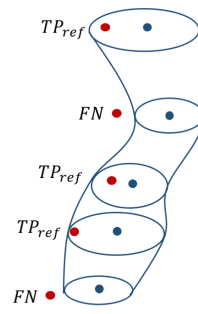
At first sight, it might seem unnatural to use true positives for both the segmentation and the reference standard. This is done because they reflect



(A) Example of how the reference (red) and segmentation (blue) could look



(B) Example of how  $TP_{seg}$  and  $FP$  are found



(C) Example of how  $TP_{ref}$  and  $FN$  are found

FIGURE 6.1: Example of how true positives, false positives and false negatives are defined

different things and using only one of them could easily be misleading. For example, let's say that only  $TP_{seg}$  is used and that the segmentation consists of only the seeding point. This would give a perfect score of  $TP_{seg}$  (because all points of the segmentation are inside the reference vessel). At the other hand, imagine using only  $TP_{ref}$  and having a segmentation that finds all points in the reference standard but continues, wrongly, marking more area in the image as coronary artery. This would yield a perfect score in  $TP_{ref}$ , even though it is apparent that the segmentation is not perfect. This is why it is important to use both  $TP_{seg}$  and  $TP_{ref}$  when calculating the overlap.

### 6.3 Tracking accuracy

As mentioned above, dataset 2 was also used to measure the tracking accuracy of the algorithm. In order to distinguish between tracking ability and tracking accuracy the accuracy was only evaluated within sections where the tracking succeeded.

The tracking accuracy was calculated as the root mean square error, RMSE, between the segmented radius and the radius of the reference standard, i.e.

$$RMSE = \sqrt{\frac{1}{n} (r_1^s - r_1^{rs})^2 + (r_2^s - r_2^{rs})^2 + \dots + (r_n^s - r_n^{rs})^2}, \quad (6.2)$$

where  $n$  is the number of valid points in the segmentation,  $r_i^s$  is the radius if the  $i$ 'th point in the segmentation and  $r_i^{rs}$  is the radius of its closest point in the reference standard.

Valid points were defined as all points where the distance from the segmentation to the closest point in the reference standard was smaller than the radius of that point in the segmentation. Points that did not qualify as valid points were not considered when calculating RMSE. This is because they were presumed not to reflect the same spot on the coronary artery as their closest point in the reference standard and thus not interesting for the result.

## Chapter 7

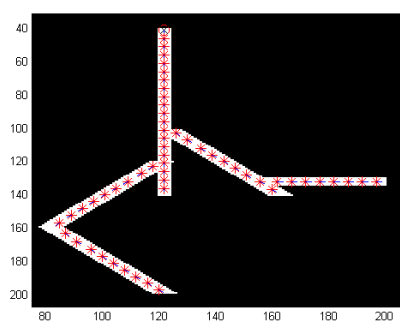
# Results

In this chapter the results from phantoms, dataset 1 and dataset 2 will be presented. All figures used for the validation of dataset 1 and 2 were in 3D but are displayed as 2D snaps of the 3D figures from a suitable angle. The computation time for the algorithm varies between approximately 3-20 minutes per seeding point.

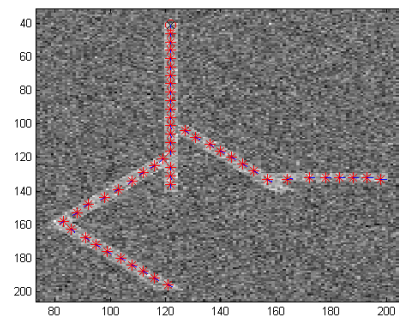
### 7.1 Phantoms

In an early stage of this master thesis manually made phantoms, with and without noise, in 2D were created and used to test the algorithm during development. These images have been included in this chapter to introduce the reader to how the development process has been conducted and also to introduce images of the results from the algorithm in 2D before expanding to 3D. These images have however not been used for the validation of the algorithm.

Some examples of results from segmentations on manually made binary phantoms in 2D with and without added noise can be seen in Figure 7.1b and Figure 7.2.

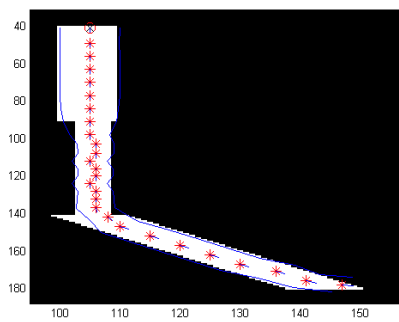


(A) No added noise

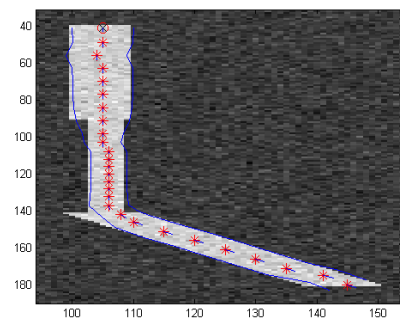


(B) Gaussian noise added with  $m = 0$  and  $SD = 0.5$ .

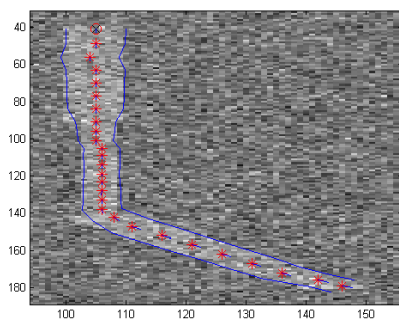
FIGURE 7.1: Segmentation on a phantom with and without noise. Each point in the final segmentation is indicated with a red star.



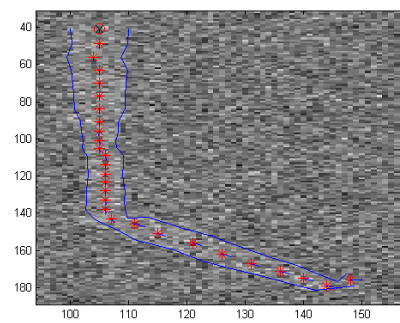
(A) No noise



(B) Noise added with SD = 0.1



(C) Noise added with SD = 0.75



(D) Noise added with SD = 1.5

FIGURE 7.2: Segmentation on a phantom with and without noise. The added noise is Gaussian with zero mean and standard deviation (SD) specified. Each point in the final segmentation is indicated with a red star. The blue lines corresponds to the estimated radius.

## 7.2 Tracking ability

### 7.2.1 Dataset 1- ability to find vessels

An example of how the reference standard and segmentation for a patient in dataset 1 could look can be found in Figure 7.3. Since dataset 1 did not contain information about the radius the plots of the reference standard has been created with a constant radius. To make the visual comparison easier,

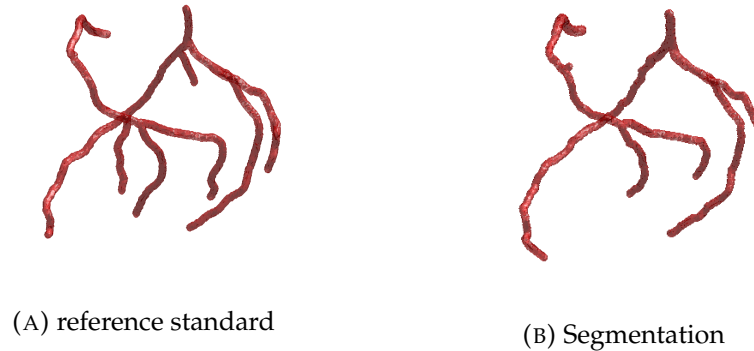


FIGURE 7.3: The reference standard and segmentation for patient 08 in dataset 1.

the reference standard and the segmentation were plotted in different colors in the same figure, this can be seen in Figure 7.4. In this figure it might look as the points of the arteries are sometimes not connected, this is not the case, it is a result from the fact that the images are 2D images of the original 3D images.

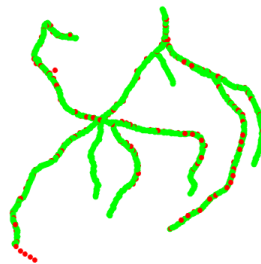


FIGURE 7.4: Visualization of the segmentation (red) and the reference standard (green) used to evaluate the algorithm. Note that the algorithm fails in finding 3 of the 8 sought for vessels.

The results of the segmentation for both the left and right coronary artery for each patient can be found in Table 7.1.

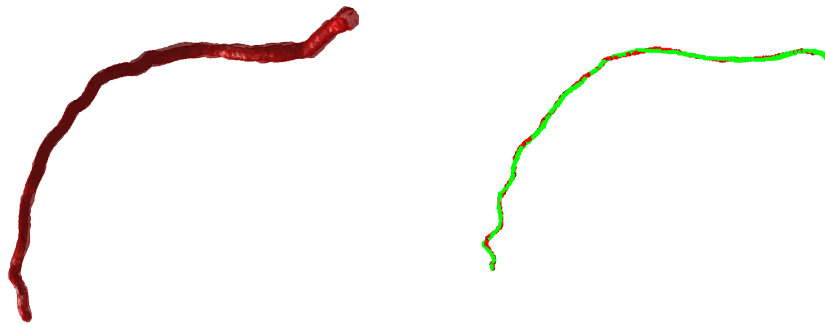
Evaluation of dataset 1			
	Nbr of branches in ref. stand.	Nbr of branches found	Match -1: shorter 0: same length 1: longer
Patient 00 Right	2	1	0
Patient 00 Left	4	3	-1, -1, -1
Patient 01 Right	2	2	0, 0
Patient 01 Left	6	5	0, 1, -1, 1, 1
Patient 02 Right	1	1	1
Patient 02 Left	5	2	0, 0
Patient 03 Right	1	1	-1
Patient 03 Left	3	2	-1, 0
Patient 04 Right	1	1	-1
Patient 04 Left	4	2	-1,-1
Patient 05 Right	2	1	-1
Patient 05 Left	4	2	-1,-1
Patient 06 Right	1	1	1
Patient 06 Left	4	2	1, 0
Patient 07 Right	1	1	-1
Patient 07 Left	4	2	1, 0
Patient 08 Right	2	2	-1, -1
Patient 08 Left	6	3	1, 0, 0
<b>Total</b>	53	34 (64%)	-1: 15 (44%) 0: 12 (35%) 1: 7 (21%)

TABLE 7.1: Table with the results for dataset 1. The second column indicates how many branches the reference standard has and the third column how many of these that are found by the segmentation. Column four indicate how the segmentation relates to the reference standard; -1: shorter, 0: same length, 1:longer.

### 7.2.2 Dataset 2 - ability to track the whole vessel

This dataset consisted of 32 coronary arteries. In seven cases, the algorithm could not find the sought for coronary artery.

Examples of segmentations can be found in Figure 7.5 and Figure 7.6. In Figure 7.7 one of the segmentations that failed can be seen. To the left in Figure 7.5-7.7, the reference standard and segmentation has been plotted in red in the same figure. To be able to distinguish between the segmentation and reference standard they have also been plotted in different colors, this can be seen to the right in Figure 7.5-7.7. In the right plots it might look as the points of the arteries are sometimes not connected, as before, this is not the case, it is a result from the fact that the images are 2D images of the original 3D images. It is also important to notice that the radii in the right plots are not according to scale.



(A) The reference standard and segmentation plotted together. (B) Reference plot, red is the segmentation and green is the reference standard.

FIGURE 7.5: Segmentation of patient 02 vessel 01 in dataset 2.



(A) Comparison between reference standard and segmentation. (B) Reference plot, red is the segmentation and green is the reference standard.

FIGURE 7.6: Segmentation of patient 01 vessel 01 in dataset 2.





(A) Comparison between the reference standard and segmentation. (B) Reference plot, red is the segmentation and green is the reference standard.

FIGURE 7.7: Patient 02 vessel 03, an example of a segmentation that failed in dataset 2.

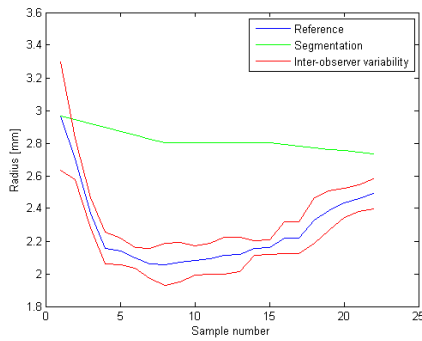
The overlap for dataset 2 can be found in Table 7.2. The overlap can vary between 0 and 1 where 0 correspond to no overlap at all and 1 correspond to perfect overlap.

Evaluation of dataset 2; The overlap (OV)				
	vessel 1	vessel 2	vessel 3	vessel 4
Patient 00	0.57	0.89	0.98	-
Patient 01	0.76	0.98	0.97	0.84
Patient 02	0.99	0.68	1	-
Patient 03	0.98	0.59	-	0.98
Patient 04	0.93	0.86	0.92	0.84
Patient 05	0.99	0.88	0.85	0.96
Patient 06	0.53	0.94	0.93	-
Patient 07	0.85	-	-	-
<b>Mean overlap</b>				<b>0.87</b>

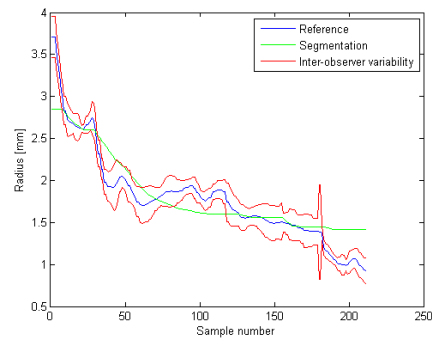
TABLE 7.2: The overlap for the segmentations in dataset 2. The overlap is calculated according to Equation (6.1). Empty boxes correspond to failed segmentations.

### 7.3 Tracking accuracy

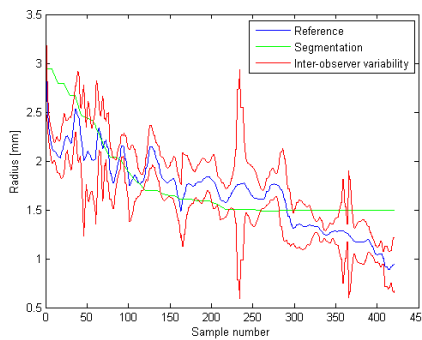
In Figure 7.8 the segmented radius (green) together with the reference standard (blue) has been plotted for four different segmentations. In the plots the reference standard  $\pm$  inter-observer variability has also been plotted (two red lines).



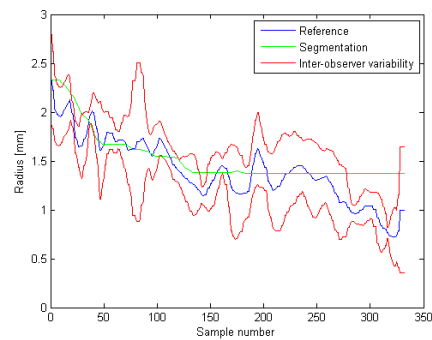
(A) Patient 01 vessel 3



(B) Patient 02 vessel 3



(C) Patient 03 vessel 1



(D) Patient 05 vessel 1

FIGURE 7.8: Comparison of the segmented radius (green) and the radius in the reference standard (blue) for different segmentations. The red interval is the radius for the reference standard  $\pm$  inter-observer variability.

The root mean square error, RMSE, of the radius for different segmentations can be found in Table 7.3. For each RMSE value in the table there is also a number in parenthesis, this is the root mean square, RMS, of the inter-observer variability for that vessel. Furthermore, some numbers are indicated in red, these correspond to segmentations that contained invalid points. The number of invalid points can be found in Table 7.4.

Evaluation of dataset 2; The root mean square of the error				
	vessel 1	vessel 2	vessel 3	vessel 4
<b>Patient 00</b>	0.74 (0.74)	<b>0.31</b> (0.31)	0.36 (0.30)	-
<b>Patient 01</b>	<b>0.25</b> (0.22)	0.26 (0.22)	0.31 (0.12)	0.48 (0.25)
<b>Patient 02</b>	0.37 (0.25)	0.89 (0.17)	0.24 (0.17)	-
<b>Patient 03</b>	0.29 (0.28)	0.30 (0.37)	-	0.44 (0.32)
<b>Patient 04</b>	0.31 (0.15)	<b>0.14</b> (0.19)	0.44 (0.20)	0.28 (0.15)
<b>Patient 05</b>	<b>0.24</b> (0.32)	0.19 (0.21)	0.23 (0.24)	0.32 (0.24)
<b>Patient 06</b>	0.14 (0.16)	<b>0.25</b> (0.17)	0.64 (0.33)	-
<b>Patient 07</b>	<b>0.24</b> (0.15)	-	-	-
<b>Mean error</b>			<b>0.30 (0.25)</b>	

TABLE 7.3: The RMSE of the radius [mm] for each segmentation in dataset 2. The numbers in parenthesis is the RMS of the inter-observer variability [mm] of the reference standard, obtained from [1]. The red numbers indicate segmentations with invalid points.

	Nbr of invalid points	% invalid points of total points
Patient 00 vessel 2	5	3 %
Patient 01 vessel 1	23	9 %
Patient 04 vessel 2	8	3 %
Patient 05 vessel 1	5	1 %
Patient 06 vessel 2	30	7 %
Patient 07 vessel 1	19	5 %

TABLE 7.4: The number of points not considered when calculating the mean error in radius for the given segmentation. The points were excluded because their spatial position was too far from the reference standard.

## Chapter 8

# Discussion and Conclusions

In this thesis an algorithm based on a vessel model and multiple hypothesis tracking scheme for segmenting coronary arteries in CT images has been presented. The algorithm has been developed in Matlab and implemented in the software Segment. The results have been validated on two different datasets obtained from the Rotterdam Coronary Artery Algorithm Evaluation Framework [1]. In this chapter the results, limitations and future work are discussed and conclusions are drawn.

### 8.1 Discussion

The results from dataset 1 indicate that the algorithm finds approximately 64% of the branches of the coronary arteries. The algorithm has been implemented so that if the user feels that the algorithm has missed branches, or has terminated early on a found branch, she/he can manually add new starting positions in the image. The segmentation will continue from these new positions and the result will be added to the final segmentation. This was not done for the evaluation because it was considered more interesting to give an idea of how much the algorithm manages to find with only one user interaction (the first seeding point).

The results from dataset 2 indicate several things. First, the mean overlap, for dataset 2 was 87%. To put this value in perspective it could be compared to results obtained during the workshop "3D Segmentation in the Clinic: A Grand Challenge II" at the 11th International Conference on Medical Image Computing and Computer-Assisted Intervention (MICCAI) in September 2008 [16]. This workshop is where the project of the evaluation framework used in this thesis began. At the workshop 13 methods for segmenting coronary arteries were evaluated with a similar dataset that has been used for the evaluation of this thesis. The mean overlap for the different methods that were competing in the MICCAI workshop varied from 67 – 98.5%, where the algorithm used as inspiration for this thesis had the highest overlap [16]. The best result from the workshop was obtained by a user interaction of 2-5 points per vessel whereas the results in this thesis were obtained with only one user interaction. Though, it needs to be emphasized that vessels that were not found by the algorithm in this thesis were excluded, which yields a higher percentage for the overlap than if they would have been included.

The results from the error in the segmented radius (both Figure 7.8 and

Table 7.3), indicate that the tracking accuracy of the algorithm is close to results achieved by manual delineation (the segmentation has a mean error of 0.3mm compared to the inter-observer variability that is 0.25mm). The results show that the algorithm manages to approximate the size of the radius on average, but that it has problems with quickly changing radius. This can be seen in the subfigures in Figure 7.8, where the segmented radius (green line) often lies within the interval created by the inter-observer variability but it is very flat compared to the radius of the reference standard (blue line) which constantly varies.

Furthermore, for dataset 2 the algorithm performs much worse for patient 7 compared to the other patients (only manages to find 1 of 4 vessels whereas in the other patients it finds 3 or 4 of the 4 vessels provided). This CT image has been studied by a specialist at coronary arteries at Skåne University Hospital in Lund and it has been established that the CT image has been taken at an earlier stage from the injection of vessel contrast injection. This resulted in a large area of very bright structures in the right chamber where the vessel contrast has accumulated, see Figure 8.1. It is probable that it has affected the performance of the algorithm.

The computation time for the algorithm varies, as was presented in the re-

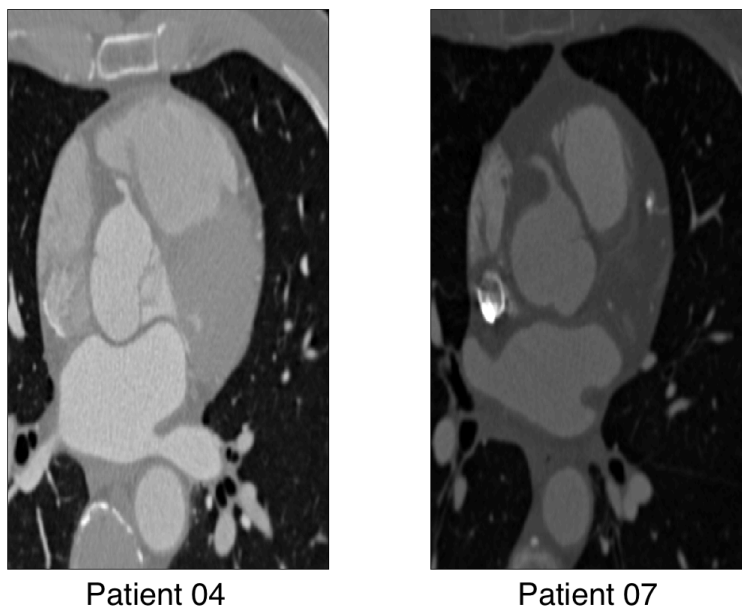


FIGURE 8.1: Comparison between patient 04 (left) and patient 07 (right) in a similar slice in the CT images from dataset 2. As can be seen, patient 07 has a bright structure to the left in the image. This is due to high concentrations of vessel contrast in that area.

sults, between approximately 3-20 minutes per seeding point. The big span in computation time is due to difference in length and number of branches of the coronary artery that is being segmented. The right main coronary artery usually has less branches than the left and thus the computational

time for the right side is usually lower.

The algorithm has been analyzed using tools for tracking execution time and the results has lead to changes in the code that improved the time efficiency of the algorithm. Due to lack of time, not all desired changes were managed to be implemented so, there are still changes that could be done to make the algorithm significantly faster and thus more interesting from a clinical point of view.

Another interesting thing to discuss is the similarities and dissimilarities between the algorithm presented and the algorithm in *Multiple hypothesis template tracking of small 3D vessel structures* [13], which it was inspired by. The algorithm is based on the same method as [13], but there are some implementational differences. Big focus has been on developing within the software Segment and thus have to adjust the algorithm to fit an already existing environment. Other differences are the parameter values and thresholds, the way of solving the non-linear differential problem when updating  $x_0$ ,  $\hat{v}$  and  $r$  and how the best predictions were chosen.

It is hard to compare the performance of the algorithms since the algorithm that Friman et al. presented was evaluated using both multiple manual inputs and also a second algorithm to segment where the MHT tracking algorithm failed while the algorithm in this thesis has only been evaluated using one manual input per vessel. One thing that could be compared though, is the computation time for the algorithms. The algorithm by Friman et al. approximately takes 6 min per coronary artery with 2-5 manual inputs, which on average is somewhat faster than the algorithm proposed in this thesis.

### 8.1.1 Limitations

One of the limitation with the algorithm proposed is that there are many parameters that needed to be assigned specific values, for example the thresholds, the angle  $\alpha$  and the length of each step used when guessing new predictions. The setup of values for these parameters that were used in the final method have been decided by testing and visual evaluation by the author. This makes it apparent that the choice of parameters is far from perfect and may be optimized to a specific dataset.

Another limitation is that the spatial position,  $x_0$ , has been chosen to be represented as pixel indices. This has been done because any other option was not considered at the beginning of the development of the algorithm. When the question arose it seemed too time consuming to change this representation throughout the whole algorithm with the given time for this project.

Another limitation of this thesis is that the update generated from `fminsearch` is not always what is sought for; sometimes `fminsearch` finds updates that are spatially somewhere else in the image or that rapidly and largely change direction and/or radius, which apparently is not the "fine-tuning" of the parameters that is wanted. Because of this, the updates need to be evaluated to see if they have been changed to what is considered

too much and if this is the case the old values are kept. This makes the algorithm miss a chance of fine tuning those vessel parameters. In addition, the threshold values are another example of values chosen in a non-optimal way since they were decided by trial and error.

### 8.1.2 Future work

As have been shown by the results and discussed in this chapter, the algorithm has problems with early termination (overlap of 87 %) and sometimes missing branches. To solve this, an approach where the user can add new seeding points after evaluating the segmentation has been implemented. This procedure is not very user friendly so far and should be further developed to make it more intuitive and easier to use.

Furthermore, sometimes the algorithm does not manage to segment the whole vessel despite adding new points. A proposition for future work is thus to implement another algorithm that could deal with these problematic vessels. An example of such an algorithm could be the minimal path approach as proposed in [13].

As has been discussed above, parameter optimization and sub-pixel spatial resolution are two things that could be of interest in the future. Another proposition is to make the algorithm start automatically instead of needing manual input. This could be done in Segment by combining this algorithm with an already existing algorithm for automatically finding the root of the aorta and the beginning of the coronary arteries.

Analyzing the execution time for the different functions within the algorithm shows that the Matlab function `fminsearch` is the most time consuming step in the algorithm. By e.g. implementing this function in the programming language C instead of Matlab, the computation time could be drastically reduced.

Furthermore, when the segmentation of the coronary arteries works better, the algorithm could be used to automatically detect stenosis and plaque in the coronary arteries and be used by medical staff when evaluating CT images of patients.

## 8.2 Conclusions

To conclude, a method based on a vessel template model combined with a multiple hypothesis tracking approach has been developed. The method has been implemented in the software Segment and it has been shown that it could be of use for the difficult task of segmenting coronary arteries.

The results show that the tracking ability of the algorithm with only one user interaction is that it finds 64% of the sought for vessels with an overlap of 87%. It has been discussed that this percentage could be higher by using more user interactions, which is a function that has been implemented in the algorithm.

The accuracy of the algorithm is close to the accuracy of manual delineation; the error of the segmentation is on average 0.3 mm compared to manual delineation which on average has an error of 0.25 mm. Though, the algorithm proposed has problems with rapid changes of the radius.

While the proposed algorithm works, there is still room for improvement. In the discussion different approaches to increase the performance of the algorithm have been proposed and even though these have not been implemented, they give a hint at what direction further development could take.





# Bibliography

- [1] Michiel Schaap et al. "Standardized evaluation methodology and reference database for evaluating coronary artery centerline extraction algorithms". In: *Medical image analysis* 13.5 (2009), pp. 701–714.
- [2] Hjärt-Lungfonden. *Hjärt- och kärlsjukdomar*. URL: <https://www.hjart-lungfonden.se/Sjukdomar/Hjartsjukdomar/>.
- [3] World Health Organization et al. "The top ten causes of death-Fact sheet N310". In: *World Health Organization, Geneva* (2008).
- [4] Hjärt-Lungfonden. *Hjärtinfarkt*. URL: <https://www.hjart-lungfonden.se/Sjukdomar/Hjartsjukdomar/Hjartinfarkt/>.
- [5] Dehkordi et al. "A review of coronary vessel segmentation algorithms". In: *Journal of medical signals and sensors* 1.1 (2011), p. 49.
- [6] Arthur J Vander and DS JH Luciano. "Humanphysiology: the mechanisms of body function". In: (1980).
- [7] *By BruceBlaus - Own work, CC BY 3.0*. URL: <https://commons.wikimedia.org/w/index.php?curid=29140356>.
- [8] National Heart Lung and Blood Institute. *What Is Atherosclerosis?* URL: <http://www.nhlbi.nih.gov/health/health-topics/topics/atherosclerosis>.
- [9] E. Heiberg J. Sjögren M. Ugander M. Carlsson H. Engblom and H. Arheden. "Design and validation of segment—freely available software for cardiovascular image analysis". In: *BMC Medical Imaging* Vol. 10, Article 1 (2010).
- [10] Chanho Kim et al. "Multiple Hypothesis Tracking Revisited". In: ().
- [11] Smith H. Draper N.R. *Applied Regression Analysis, 3rd ed.* 1998.
- [12] Fan RK Chung. *Spectral graph theory*. Vol. 92. American Mathematical Soc., 1997.
- [13] Ola Friman et al. "Multiple hypothesis template tracking of small 3D vessel structures". In: *Medical image analysis* 14.2 (2010), pp. 160–171.
- [14] MathWorks. *Optimizing Nonlinear Functions*. URL: <http://se.mathworks.com/help/matlab/math/optimizing-nonlinear-functions.html#bsgpq6p-11>.
- [15] Lee R. Dice. "Measures of the Amount of Ecologic Association Between Species". In: *Ecology* 26.3 (1945), pp. 297–302. ISSN: 00129658, 19399170. URL: <http://www.jstor.org/stable/1932409>.
- [16] Coert Metz et al. "3D segmentation in the clinic: A grand challenge ii-coronary artery tracking". In: (2008).

Master's Theses in Mathematical Sciences 2016:E13

ISSN 1404-6342

LUTFMA-3291-2016

Mathematics

Centre for Mathematical Sciences

Lund University

Box 118, SE-221 00 Lund, Sweden

<http://www.maths.lth.se/>